Progress In Electromagnetics Research B, Vol. 66, 15–29, 2016

Practical Investigation of Different Possible Textile Unit Cell for a C-Band Portable Textile Reflectarray Using Conductive Thread

Muhammad M. Tahseen* **and Ahmed A. Kishk**

Abstract—Investigation of a unit cell in terms of reflected wave amplitude and phase, for designing linearly polarized single layer Textile-Reflectarray (TRA) at C-band, is presented. The relative dielectric constant of the material is extracted using resonance method, and a WLAN antenna is designed to verify the accuracy of extracted material parameter. An error of 5% is observed in the extracted dielectric constant, when performance of WLAN antenna is measured at WI-FI Band (2.4 GHz). The extracted dielectric constant is used in the unit cell designing for TRA at the C-band (5.8 GHz). The radiating element is made using laying technique with conductive thread. A square patch with a ring is selected after analyzing multiple geometries of the patch providing the required reflected phase range and low losses. By varying size of patch and ring of single layer unit cell in CST periodic environment, reflected phase range of 360 degrees is achieved, which is required for reflectarray (RA) designing. The solid copper ground plane at the bottom of unit cell is replaced with conductive shielded fabric with high level signal attenuation. Four different sizes of textile unit cells are fabricated using conductive thread, and the reflected phase and amplitude are measured using waveguide method. The simulated and measured results are compared when solid copper ground plane at the bottom of unit cell has been replaced with shielded fabric. The proposed method provides the first step towards designing flexible high gain textile reflectarrays.

1. INTRODUCTION

Certain wireless applications require high gain antennas especially for long distant communication systems. Some of the antennas, such as parabolic reflectors and array, fulfill the requirement but has some drawbacks [1]. Parabolic reflectors have curved shape and bulky in size, which makes them difficult to fabricate while the traditional arrays require complex feeding network, which are difficult to design for large arrays operating at high frequencies. These feed transmission lines increase the antenna losses and cause undesired radiations which affect the overall antenna performance [2]. Reflectarrays are recently proposed as an alternative to both parabolic reflectors and arrays, which have low cost, light weight and easy design [1, 2].

RA works on the principle of geometrical optics (GO). The incident wave with spherical wave front, transmitted from the prime feed at focal point, is converted to planar wave front at RA surface in transmit mode while converting back the planar wave front to spherical wave front in receiving mode, focusing the energy to a focal point of reflector. The elements at the RA surface are designed subject to the compensated required path delay at that location. In [2], this phase compensation objective is analyzed by size variation of the elements for linearly polarized antenna while in [3], it is achieved by element rotation for circularly polarized antenna. Both the techniques result in some tradeoffs along with there benefits. In [4, 5], it is analyzed that increasing the phase range with minimum slope variation provides wider bandwidth and less fabrication tolerance. Multiple geometries of the radiating elements

Received 17 September 2015, Accepted 21 January 2016, Scheduled 9 February 2016
* Corresponding author: Muhammad M. Tahseen (m_tahse@encs.concordia.ca).
The authors are with the ECE Department, Concordia University, Montreal, Canada.

are analyzed in unit cell environment [6], for phase characteristics only where the amplitude losses are not considered due to low-loss ceramic materials usage. Several RA are analyzed and fabricated using veracious elements mostly using ceramic materials. In [7], cross slot rotation technique has been used for multilayer circularly polarized (CP) RA antenna design. The stacked elements in [8] and multilayer coupled resonance elements in [9, 10] have been used. Each technique provides some advantages and some tradeoffs, due to multiple factors explained in their work. In [11], it is described that RA bandwidth is mainly affected by two major factors, element bandwidth and the path difference between elements, and by minimizing these barriers, bandwidth can be increased. It is effective to get wide RA bandwidth, and single layer array elements designs with multi-coupled resonance elements are analyzed for widening the bandwidth, in [12, 13].

A novel flexible RA unit cell is proposed in this paper using textile materials. All previous published reflectarrays are designed using ceramic materials, which are expensive and do not have flexibility. The textile materials are being used extensively for designing antennas for medical and wearable applications [14–17]. To use fabric as a substrate in RA, electrical properties of the used material should be known. There are certain methods used for extracting material properties e.g., coaxial probe method [21], waveguide method [22], cavity method [23], free space method [24], resonance method [25] and ridge-gap waveguide method [26]. The relative permittivities of the samples under test are extracted and validated by resonance method, which is further used in designing textile RA unit cell. The textile materials used in RA provide advantage over non-flexible in portability and low cost. A comprehensive investigation of the unit cell in terms of reflected wave amplitude and phase is done in this paper. The single element in a RA is simulated in CST unit cell periodic environment. The unit cell has size of $0.55\lambda \times 0.55\lambda$. The reflected wave amplitude and phase curves are obtained by varying the size of radiating element made by conductive thread. The proposed method is prominent compared to previous published methods in the case of portability, low cost, wide gain bandwidth, in LP RA antennas.

2. TEXTILE MATERIAL SELECTION CRITERIA AND RELATIVE PERMITTIVITY EXTRACTION

2.1. Samples Under Test (SUT)

To use fabric as a substrate in RA designing, multiple samples with different material compositions are selected for this investigation. It is observed that not every textile material is suitable for wearable antenna designing as well as RA designing. Among all tested textile materials, four samples are selected and shown in Figure 1(P1), depending on thickness and elasticity. Sample 1 in SUT is a non-woven synthetic bonded-fiber fabric. Its thickness is regular. It is also easy to sew, non-tearable and will not crease, composed of 100% polyester. Sample 2 is a light plain woven 100% cotton fabric. It is made of woven cotton yarn. It is very resistant, easy to sew but will crease. Usually, in order to strengthen it and keep it flat during the laying process, we double it with tearable interfacing fabric (Sample 3). Sample 3 material, with 50% cotton and 50% polyamide for backing, is a thin non-woven tear-away interfacing polyester fabric used as described above. Sample 4 is a looser plain woven 65% polyester and 35% cotton mix. Sample 3 must be used as a backing material every time during the laying process. The SUT are suitable for designing wearable antennas, as these are solid with less elasticity, helping in tighten wovening. If SUT are highly elastic, their properties may get disturbed during wovening and after releasing from the laying machine.

2.2. Thickness Measurement Gauge for Textile Materials

The accurate thickness measurement for the fabric material is very critical. Most of the textile materials have very low thickness, and stacking multiple layers is necessary to meet the required substrate thickness. As the fabric is soft, the measurement of stacking layers is a problem unless the SUT is thick enough where the percentage error is minimum. To measure the thickness of SUT accurately, standard available gauge is used shown in Figure 1(P2), where the calibration is done when two metal plates are connected with full pressure on upper piston towards bottom plate. In Figure 1(P2), Sample 1 is used to measure the thickness, resulting in 3.2 mm, and same procedure is repeated on other samples.

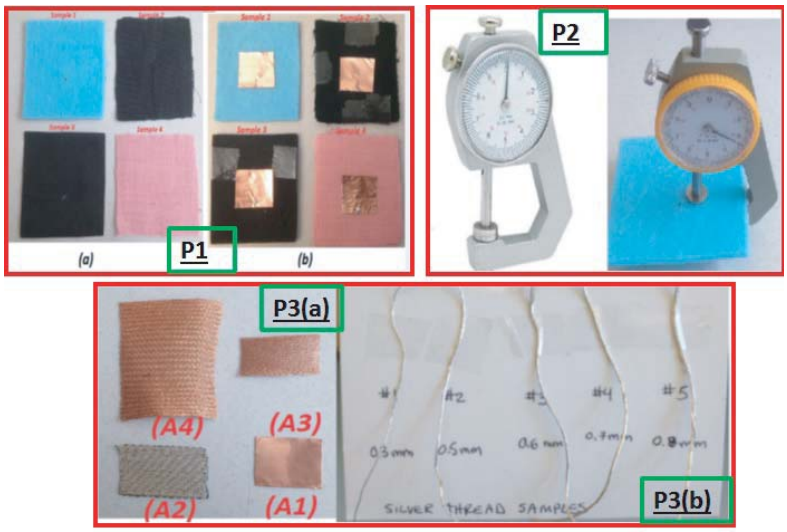

Figure 1. (P1) Samples Under Test (SUT), (P1a) four tested samples, (P1b) samples with patch, (P2) thickness measurement device, (P3) conductive materials.

2.3. Conductive Threads the Suitable Substitute for Copper Sheets

There are several conductive materials that can be used for designing radiating elements as shown in Figure 1(P3). The conductivity of each material varies depending on its composition. In Figure 1(P3a), A1 material is conventional copper with the highest possible conductivity while A3 and A4 are stretchable meshed conductive grids with two available strip sizes. The conductivities of these materials are also very close to conventional copper sheet, as the strips are made with very thin copper wires meshed together with air-gaps present in between wires, when strip is non-stretched. But when strip is stretched to be used as required radiating element dimensions, air-gaps between grids increase, and it is difficult to maintain the same stretch everywhere, causing variable air-gap between thin copper wire grids. This variable air-gap generates capacitive effect, reducing the electrical resistivity, which results in resonant frequency shift. A2 material is a fabric type of multi-stranded conductive strip, with low conductivity compared with conventional copper and A3, A4 samples. This material is less stretchable than A3 and A4 because non-conductive threads are sewn in the grid format on its back side while front side is shiny due to silver coated thin conductive threads arrangement. In Figure 1(P3b), several silver coated conductive threads are shown with variable sample diameters starting from 0.3 mm to 0.8 mm. Each conductive thread is an array of sub-thinner silver coated threads, rolled together resulting in the overall thread diameter, respectively. The conductive thread Sample 1 in Figure 1 (P3b), with particular calculated conductivity of 3.6×10^6 S/m, is used in designing TRA unit cell. This calculated conductivity of silver coated threads is almost 9.41%, less than both conventional copper (5.813×10^7 S/m) and silver (6.173×10^7 S/m) materials' conductivity. It is important to mention that dealing with large diameter conductive threads in laying process or embroidery is very difficult in shaping the required corner bends present in antenna designs.

2.4. Relative Permittivity Extraction for Sample Under Test

Using fabric material in RA design, the electrical properties of the textile material should be known. The relative permittivities of SUT are extracted using resonance technique [25]. The four individual patch antennas with each SUT are designed at 5 GHz as shown in Figure 1(P1b). The patch antenna dimensions at 5 GHz are calculated using Equations (1) to (5). According to the literature review, in most of the designed wearable and flexible antennas using fabric, material dissipation factor (loss tangent) lies within 0.005–0.02 [14–20]. The material maximum dissipation factor 0.02 is used in this

unit cell analysis paper.

$$W_p = \frac{c}{(2f_c)}\sqrt{\frac{2}{(\varepsilon_r+1)}} \tag{1}$$

$$\varepsilon_{eff} = \left[\frac{\varepsilon_r+1}{2}\right] + \left[\frac{\varepsilon_r-1}{2}\right]\left[1+\frac{12h_{sub}}{W_p}\right]^{-\frac{1}{2}} \tag{2}$$

$$L_p = \left[\frac{c}{(2f_c\sqrt{\varepsilon_{eff}})}\right] - 2\Delta L \tag{3}$$

$$\frac{\Delta L}{h_{sub}} = 0.412\left[\frac{(\varepsilon_{eff}+0.3)}{(\varepsilon_{eff}-0.258)}\right]\left[\frac{(\frac{W_p}{h_{sub}}+0.264)}{(\frac{W_p}{h_{sub}}+0.8)}\right] \tag{4}$$

$$L_{eff} = L_p + 2\Delta L \tag{5}$$

where W_p is the patch width and L_p the patch length calculated at center frequency f_c of 5 GHz. The simulated and measured reflection coefficients using each SUT are shown in Figure 2. The new measured resonant frequency for each SUT is used in extracting relative permittivities of the samples summarized in Table 1. The accuracy of the extracted dielectric constants of SUT should be authenticated before using them in unit cell design so validation is made, explained in the upcoming section.

Table 1. Extracted relative permittivities of samples under test.

SUT	Extracted ε_{eff}	Extracted ε_r	Error (%)
Sample 1	1.46	1.51	2.1
Sample 2	1.39	1.45	2.6
Sample 3	1.18	1.21	10.1
Sample 4	1.37	1.41	5.7

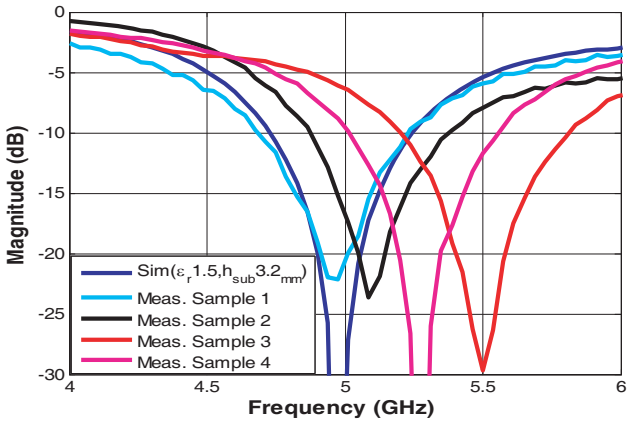

Figure 2. Relative permittivity extraction for samples under test using resonance method.

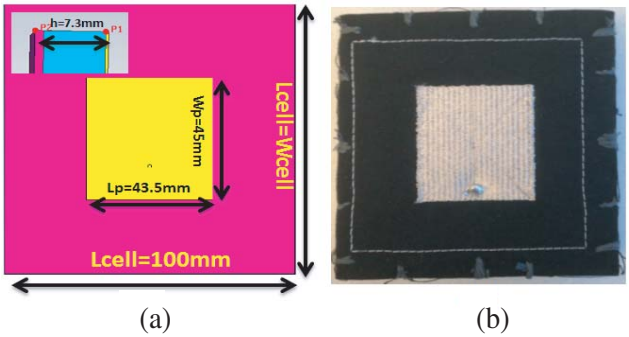

Figure 3. WI-FI band patch antenna design for the extracted relative permittivity validation.

2.5. Validation for Extracted Relative Permittivity

To verify the accuracy of extracted material permittivity, three different methods are used. In the first validation method, a WLAN WI-FI band wearable antenna is designed and measured at 2.45 GHz,

while in the second method, IEEE C-band compact size patch antenna with symmetrical radiation in both planes is designed and measured at 5.8 GHz. The objective for designing the C-band compact size patch is to use it as a feed in textile-based RA, where symmetrical radiation pattern is preferred for low cross polarization and compact size feed to reduce the blockage due to the feed. In the final algorithm verification method, a standard available foam material with known relative permittivity and thickness is used in designing WLAN band antenna at 2.45 GHz and measured.

2.5.1. Antenna Design for WI-FI Band for Wearable Applications

In the first extracted material verification method, a WLAN band wearable antenna is designed, using conductive thread. The simulated and fabricated laid antennas are shown in Figures 3(a), (b). Sample 1, Sample 2, and Sample 3 are selected to be used in the design, for their material composition as explained in the previous Section 2.1. Sample 2 is used as a backing material as it is more suitable for the laying machine. The simulation and measured results at 2.45 GHz are shown in Figure 4. The shift in the measured resonant frequency has many possible reasons such as possible error in fabricated patch dimensions, which lies within 1% in patch length shortage and possible small air-gap between layers that might be another reason. It is promising to mention that the error is 2.1%, between simulation result using extracted material properties and the measurements.

2.5.2. Replacing Solid Ground Plane with Shielded Fabric

In this section, flexibility analysis is done by replacing solid copper ground plane used in the previous WLAN antenna with the shielded fabric ground plane as shown in Figure 5. The used shielded fabric consists of hot melt adhesive backing for sticking with textile material. According to the data sheet of the material (Cat. # 1220, LessEMF) [27], it is high quality flame retardant fabric (UL 94V-0) for radio frequency and microwave shielding. The thickness of this material is 0.17 mm. This was made with particles of rugged rip-stop polyester substrate (for superior strength and handling), conductive Nickel and Copper plated (for excellent shielding and low corrosion). Later, this material is coated on one side with a non-conductive hot melt adhesive (which activates at 130°C = 266°F), which is not damaging even it is ironed onto cotton, wood, glass, paper, or rolled on a tube. This is highly suitable in RA design. Beside this the shielded fabric material has one-sided surface resistivity < 0.5 ohm/sq. and can be sewn like an ordinary fabric. The material offers shielding performance (> 60 dB) from 10 MHz to 3+ GHz, and it blocks virtually all ELF & VLF electric fields when used as a ground plane. The comparison between simulated and measured results with solid and shielded fabric ground planed is shown in Figure 6. It can be observed that the resonance frequency is shifted when the shielded fabric is used as a ground plane compared with the solid ground plane. The resonant frequency shift

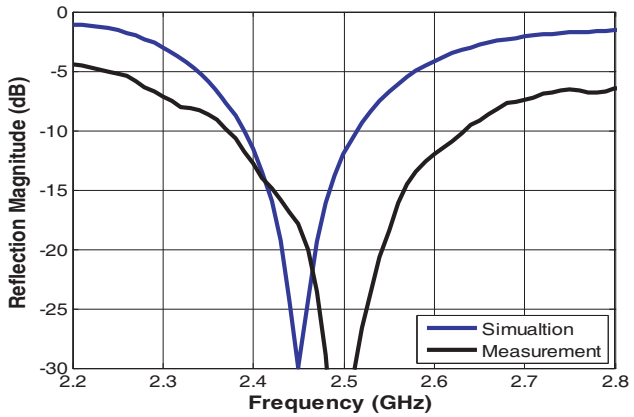

Figure 4. Simulation and measurement of the WI-FI band patch antenna for permittivity validation.

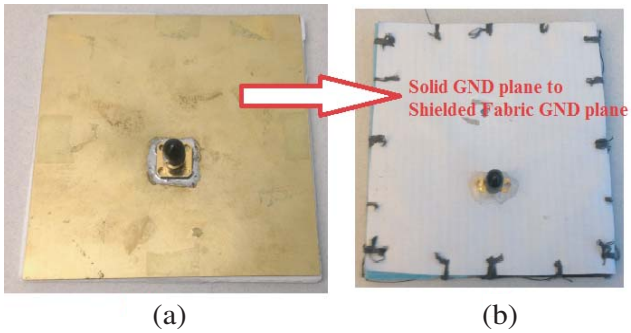

Figure 5. Replacing solid ground plane with shielded fabric ground plane.

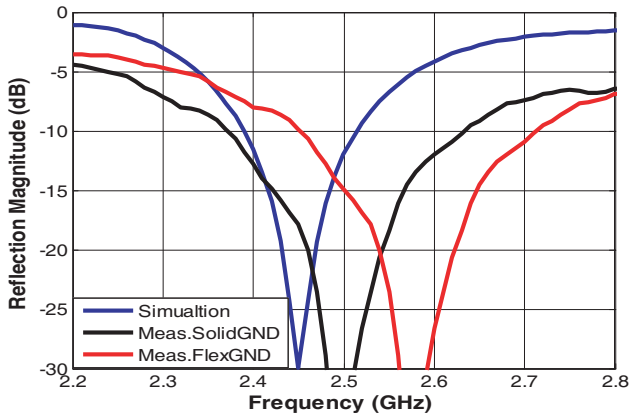

Figure 6. WI-FI band antenna's simulation and measurement results comparing solid ground and shielded fabric ground plane.

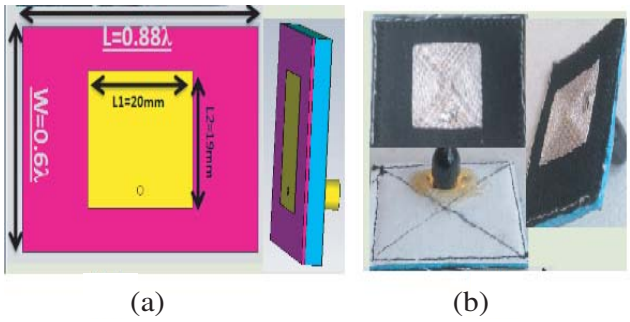

Figure 7. IEEE C-band antenna simulation and prototype.

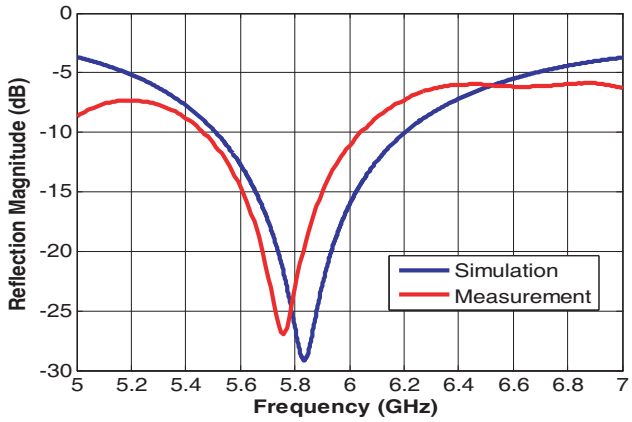

Figure 8. IEEE C-band patch antenna simulation and measurement results.

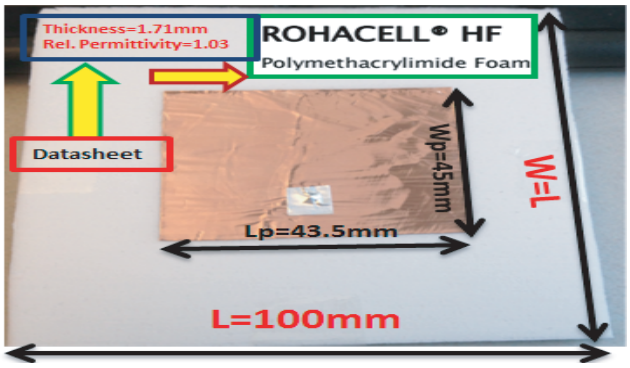

Figure 9. WI-FI band patch antenna at 2.45 GHz using standard available foam material.

is probably due to non-flatness of the ground plane and the possibility for air-gap, which still exists between textile layers.

2.5.3. Antenna Design for IEEE C-Band Using Conductive Thread

An IEEE C-band, compact size laid patch antenna, with symmetrical radiation in both planes, is designed and fabricated for validation of the extracted relative permittivity. The designing frequency is 5.8 GHz. The objective for designing this antenna is to use it as a feed later in textile RA. The ground plane dimensions are optimized to get symmetrical radiation pattern in both planes, which is desirable for the feeds used in RA or in parabolic reflectors excitations. The symmetrical radiation pattern of the feed decreases cross polarization of RA while the compactness reduces feed blockage. The simulated and fabricated C-band laid patch antennas with shielded fabric used as the ground plane are shown in Figures 7(a) and (b). The designed antenna is fed by a standard 50 Ω coaxial cable on the bottom side resulting in broadside radiations. The simulated and measured results in terms of reflection coefficient are shown in Figure 8. The C-band antenna is designed to resonate at center frequency 5.8 GHz while the measured resonant frequency is 5.75 GHz, resulting in near 1% error, which again validates the accuracy of the extracted material properties used in the design.

2.5.4. Validation Through Standard Available Material

A WLAN patch antenna is designed and fabricated (at 2.45 GHz), using standard available material with known relative permittivity and thickness as shown in Figure 9. The used dielectric material is ROHACELL polymethacrylimide foam with thickness 1.71 mm and dielectric constant of 1.03. The simulated and measured results are shown in Figure 10. The measured resonance frequency is used in the algorithm explained in Section 2.4, to extract the relative permittivity. The effective dielectric permittivity of antenna with foam is measured 1.09 while the relative permittivity is extracted 1.10 with an error of 6.6%, between simulation and measurement results. This error is possibly due to imperfect copper tape radiating patch position or the unwanted ripples created during sticking copper tape at the foam upper surface. These validation methods encourage using SUT in textile RA designing with extracted relative permittivity mentioned in Table 1.

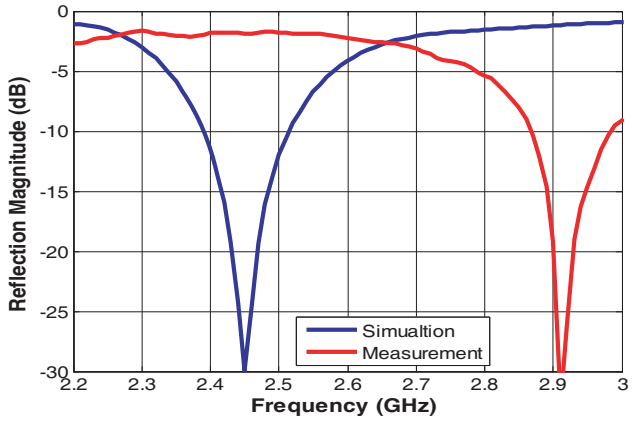

Figure 10. Simulation and measurement for the standard available foam material.

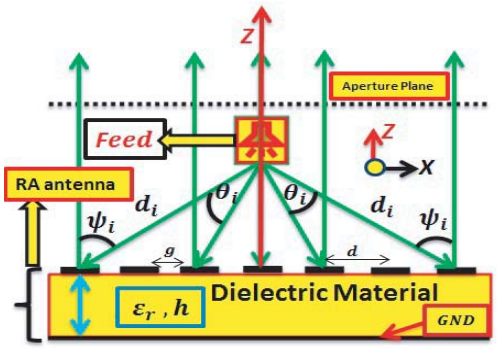

Figure 11. Reflectarray basic principle.

3. UNIT CELL ANALYSIS FOR TEXTILE-REFLECTARRAY (TRA)

Multiple elements are arranged on a substrate in such a manner that each element is subjected to reflecting a particular phase, needed to compensate spatial delay, as shown in Figure 11. An incident field with spherical wavefront travels from the feed, placed at the focal point, towards RA surface and is converted to planar wave-front after reflection from the surface. This incident field, when hits the RA surface, generates surface current at each striking location on the surface where elements are excited, and this phenomenon generates reflected fields. Each element in the array contributes its energy in converging towards desired direction. The field is incident on each element in RA at certain angle e.g., normal and oblique incidences. The constant scattered field phase can only be obtained from RA, if proper phase compensation is made to individual elements.

3.1. Reflected Wave Characteristics of Circular and Square Patches

In order to investigate RA unit cell in terms of reflected wave amplitude and phase, circular and square patch elements are used. y-polarized plane wave is used to excite the unit cell element, placed in a periodic boundary condition along X and Y directions. The square and circular patches are analyzed with two possible thicknesses as shown in Figure 12(A), where the thickness is extended using 2 mm stacked layers of Samples 2 & 3. It is observed that without using supporting extended layer in between, the reflected wave phase range remains almost the same in both circular and square patches while the losses are near -0.8 dB, when patch size is varied between 14 mm to 25 mm. Using a middle extra layer reduces the sharp amplitude losses for smaller element sizes (15–19 mm), which will exist in final RA distribution, but this extra layer reduces the overall reflected phase range of the element from 240° to 185° in both circular and square patch elements. As we are concerned with the reflected wave phase

curve's slope, both shapes are lower in slope variation, which helps in reducing fabrication tolerance. The minimization in the amplitude losses is an important parameter in the textile RA design to obtain higher antenna performance in terms of aperture efficiency and wider bandwidth. This extra supporting layer is added in unit cell thickness for further analysis while analysis is continued to other geometries until the objective of required reflected phase range (near or over 360° degree) with low amplitude loss is achieved. The results in terms of reflected wave amplitude and phase, without extra layer and with extra supporting layer, are shown in Figures 13 to 14.

3.2. Reflected Wave Characteristics of Single and Multiple Dipoles

Single and multiple size varying dipole elements are investigated in this section. Three different geometries, as shown in Figure 15, are used to obtain the reflected wave amplitude and phase characteristics. In Figures 15(a), 15(b), and 15(c), the dipole width of 4 mm is used while the gap of 2 mm is used between dipoles in Figures 15(b) and 15(c). The dipole width and gap between dipoles can further be analyzed to get the effect of these parameters on reflected wave characteristics, which are not shown here for brevity. A maximum reflected phase of 275° degrees with smooth phase slope is obtained when multiple dipole elements with different sizes are used as radiating element. The reflected

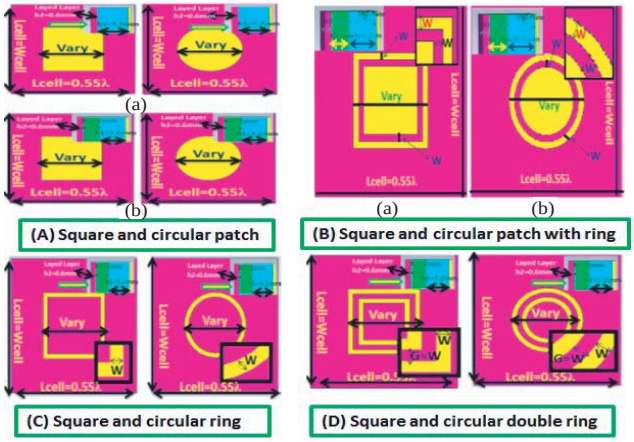

Figure 12. (A) Square and circular patches unit cells, (B) square and circular patch with ring unit cells, (C) square and circular ring unit cells, (D) square and circular double ring unit cells.

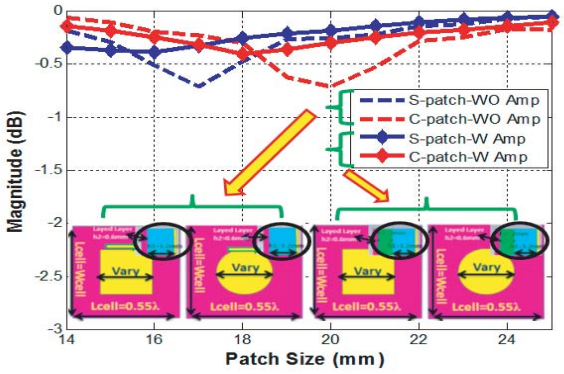

Figure 13. Spatch and Cpatch unit cell amplitude curves with and without middle supporting fabric substrate at 5.8 GHz.

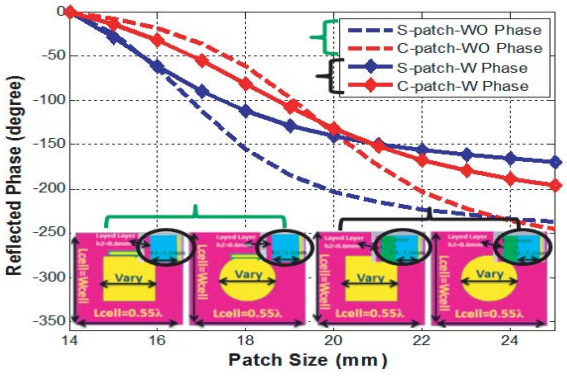

Figure 14. Spatch and Cpatch unit cell phase curves with and without middle supporting fabric substrate at 5.8 GHz.

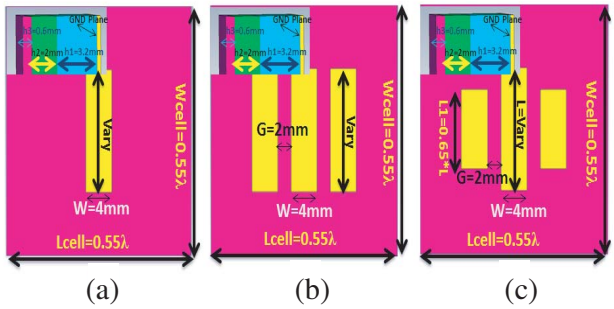

Figure 15. Dipole unit cells, (a) single dipole, (b) multiple dipoles with same length, (c) multiple dipoles with different length.

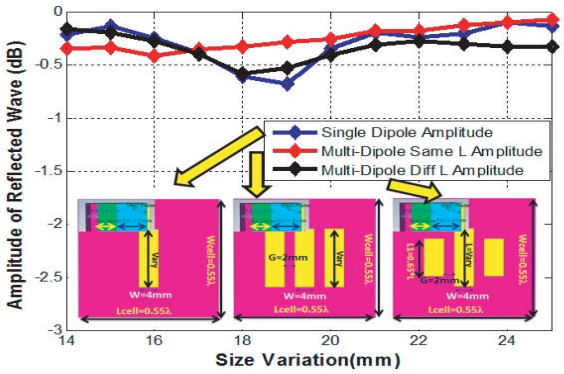

Figure 16. Reflected wave amplitude comparison at 5.8 GHz, (a) single dipole, (b) multiple dipoles with same length, (c) multiple dipoles with different length.

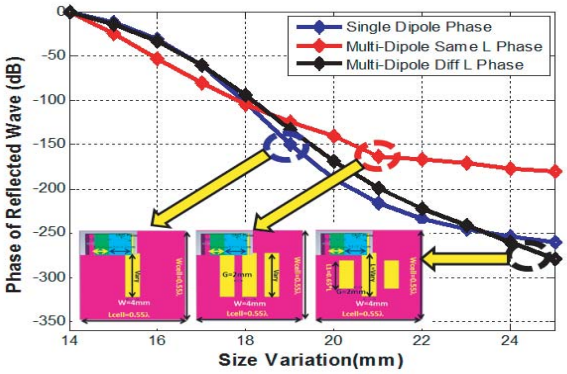

Figure 17. Reflected wave phase comparison at 5.8 GHz, (a) single dipole, (b) multiple dipoles with same length, (c) multiple dipoles with different length.

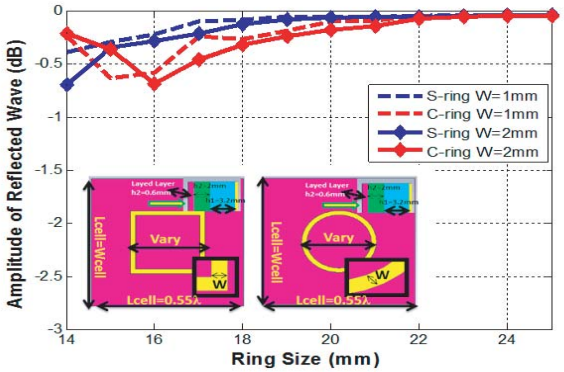

Figure 18. Sring and Cring Amplitudes comparison with ring width and gap variation at 5.8 GHz.

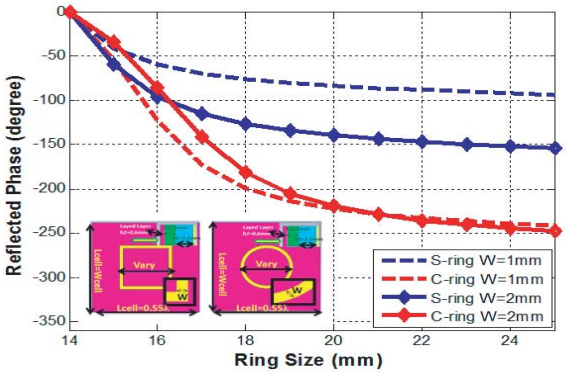

Figure 19. Sring and Cring phase curves comparison with ring width and gap variation at 5.8 GHz.

wave amplitude from multiple sizes varying dipole is around 0.6 dB. The performance from each dipole geometry is compared in terms of reflected amplitude and phase, as shown in Figures 16 and 17.

3.3. Reflected Wave Characteristics of Circular and Square Single Rings

The analysis is continued for single square and circular shapes ring elements as shown in Figure 12(C). The ring width is initially set to 1 mm for both square and circular shapes and later changed to 2 mm for observing the amplitude and phase curve behavior with ring width variation. It is quite interesting to mention that the total reflected wave amplitude loss and phase range remain almost the same for circular ring size variation and almost no effect by changing the ring width while the square ring amplitude losses are less affected, but the phase range increases as the ring width is increased, as shown in Figures 18 to 19. The objective of required reflected phase with complete 360° cycle has not yet been achieved, so the analysis continues.

3.4. Reflected Wave Characteristics of Circular and Square Double Rings

As it has been observed by the results presented in the two previous cases, the reflected phase curves from single-layer laid square and circular patches or single square and circular rings do not satisfy the requirement of low phase slope with full 360° degrees range. To counter this problem, double square and

circular laid elements are analyzed. These double rings increase the reflected phase range by creating dual-coupled resonance when the gaps between rings and ring widths are optimized for strong coupling. The double square and circular ring elements are shown in Figure 12(D), where the gap between two rings is equal in size with the ring width. The results show that the required phase range of full 360° is obtained in both elements when the ring width and gap between them is 1 mm or 2 mm. It can be seen by the comparative results in terms of amplitude and phases, shown in Figures 20 and 21, when square double ring elements have equal ring width and gap between rings at 1 mm, the total reflected phase range is over 400° while the amplitude losses with this design reaches near 1.5 dB. When the ring width and gap is changed to 2 mm, the element is suitable for TRA design, resulting in phase range of approximately 500° degrees with good phase slope, and the amplitude losses are decreased to 1 dB. On the other hand, double circular ring with ring width and gap equal to 1 mm shows strong coupled resonances between two resonance rings and results in the total phase range near 590° with amplitude losses near 1 dB, and when the ring width and gap is changed to 2 mm, the phase range decreases to 480° due to decrease in the coupling between rings while the overall amplitude loss remains near 1.2 dB. It is important to mention here that some of the element size range, in double square and double circular unit cell, results in sharp amplitude losses and higher phase slope, which is strongly undesirable in RA design due to fabrication tolerance and losses because these elements result in decreasing overall RA antenna performance. These double square and circular rings can be used in textile RA design, but due to the usage of conductive thread, it will be extremely difficult to get the same ring width, gap width, and accurate corner bends, in laid RA. Small error in these parameters, in the fabricated RA, will collectively degrade the overall antenna performance. It is suggested to use elements with higher thread density, which will result in a smooth current flow on the surface, reducing the possible tolerance errors and in return providing better antenna performance.

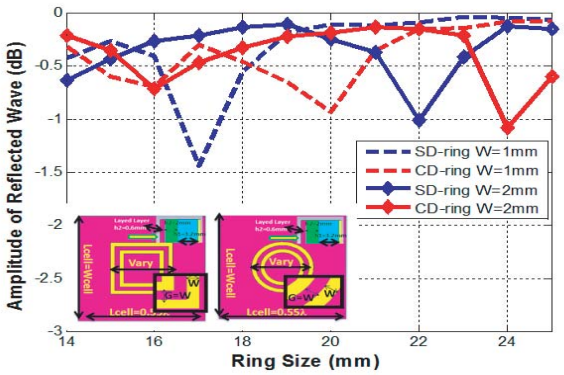

Figure 20. Reflected amplitude comparison with ring width and gap variation in double square and circular rings unit cell at 5.8 GHz.

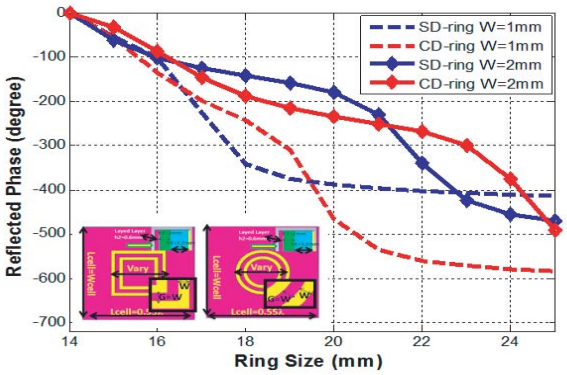

Figure 21. Reflected phase comparison with ring width and gap variation in double square and circular rings unit cell at 5.8 GHz.

3.5. Reflected Wave Characteristics of Circular and Square Single Rings with Patches

In this section, combinations of patch and ring shapes are analyzed in unit cell environment. A square patch with square ring and a circular patch with circular ring, as shown in Figure 12(B), is investigated for reflected phase and amplitude. Initially, the ring width and the gap between ring and patches are made equal to 1 mm, and results are obtained while in the second case, these parameters are changed to 2 mm, analyzing the effect of reduced coupling on the phase curves. The obtained results, shown in Figures 22 to 23, are very promising as amplitude losses are less than −0.7 dB, and phase range is also near 360° while the element with circular patch and circular ring provides phase range near 480°, when the equal ring width and gap is used at 1 mm. Maintaining this 1 mm gap between ring and patch is extremely difficult in laying RA elements because conductive thread and machine needle's diameter may cause physical contact between ring and patch. So a minimum value of 2 mm or more is recommended in textile RA design to overcome these fabrication limitation problems and to get accurate antenna results.

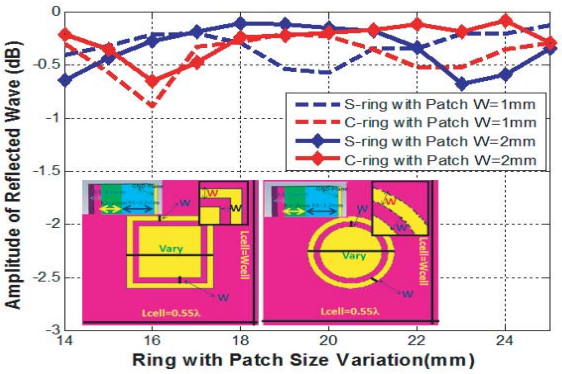

Figure 22. Reflected amplitude comparison with ring width and gap variation in square patch with ring and circular patch with ring unit cell at 5.8 GHz.

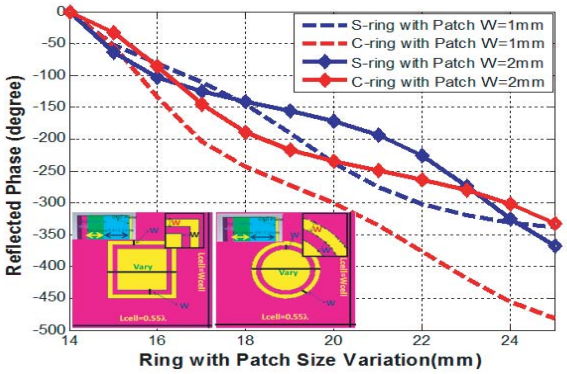

Figure 23. Reflected phase comparison with ring width and gap variation in square patch with ring and circular patch with ring unit cell at 5.8 GHz.

Table 2. Summary of analyzed unit cells in terms of reflected wave characteristics at 5.8 GHz.

		Amplitude Loss (dB)	Refl. Phase (degrees)
Spatch/Cpatch	Spatch	−0.4	160°
	Cpatch	−0.4	195°
Dipoles	Single	−0.7	260°
	Three (Same L)	−0.4	182°
	Three (Diff L)	−0.6	275°
Sring/Cring	Sring ($W = 2$ mm)	−0.7	160°
	Cring ($W = 2$ mm)	−0.7	250°
SDring/CDring	SDring ($W = 2$ mm)	−1	480°
	CDring ($W = 2$ mm)	−1.1	490°
SRingPatch/CRingPatch	SRpatch ($W = 2$ mm)	−0.7	360°
	CRpatch (2 mm)	−0.7	335°

The reflected wave characteristics of all analyzed unit cells are summarized and shown in Table 2, where the unit cell in red color is selected for the RA design in C-band (at 5.8 GHz).

Several novel unit cells are analyzed, as shown in Figure 24, but none of them provide the 360° reflected phase and low amplitude losses, required for RA design, so there results are not shown here for brevity. It has been observed during the unit cell investigation that only the coupled resonance elements provide the necessary RA design parameters. The immovable parameters in textile RA unit cell, e.g., extracted dielectric constant, fabric thickness, and the commodious unit cell size for avoiding grating lobes when over-sized, are the handicaps in providing wider reflecting phase range and low amplitude losses. These material parameters are not fixed in all the RA design, presented in [1–25], where some of the researchers have used air gaps in between the unit cell layers for satisfying the required reflected phase and making the curve linear. The air gaps in the proposed techniques are avoided because of possible difficulty in maintaining the actual air gap in fabricated RA that will further deteriorate the TRA performance, and the layers flatness problem may also occur when layers are separated.

The square patch surrounded with ring is selected for TRA design due to low amplitude loss and a complete 360° reflected phase cycle, as shown in Figure 25.

3.6. Prototype for Analyzing Possible Fabrication Problems and Measurements

A prototype is made for evaluating the possible fabrication limitations and problems. The possible source of errors in fabrication may come from, e.g., wrong ring width, gap between patch and ring,

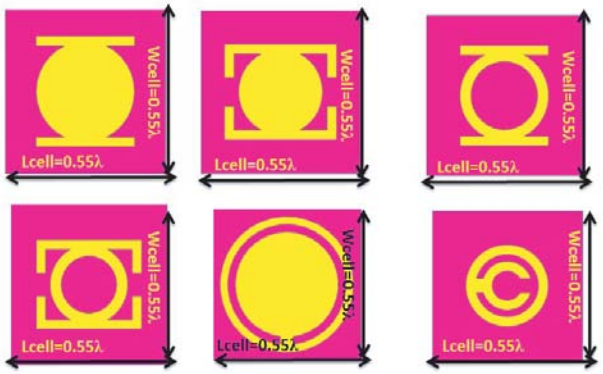

Figure 24. Several novel unit cells are analyzed for textile RA design at 5.8 GHz.

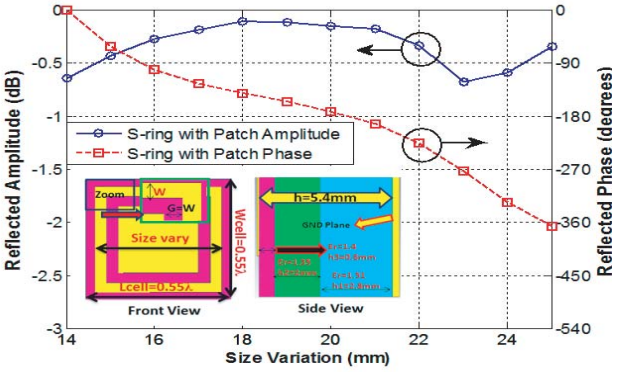

Figure 25. Reflected wave amplitude and phase of the selected unit cell for TRA design at 5.8 GHz.

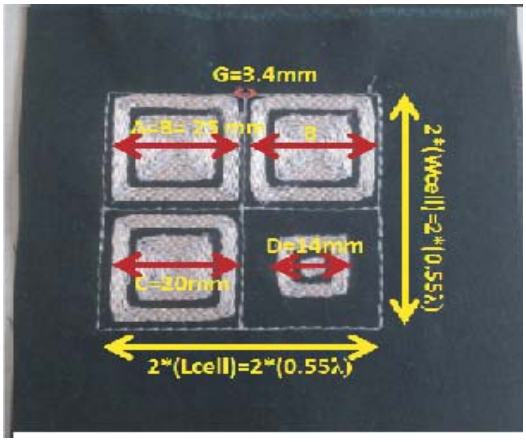

Figure 26. Four elements prototype analysis of TRA using conductive thread.

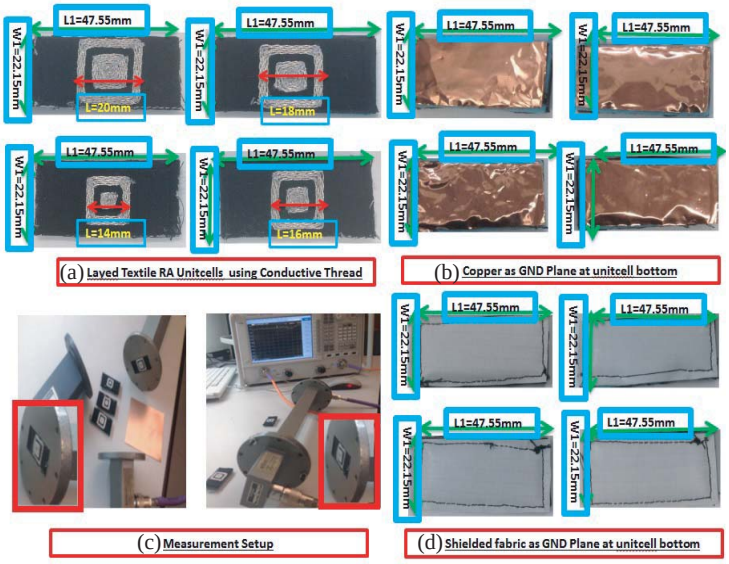

Figure 27. (a) Laid unit cells using conductive thread, (b) copper as ground, (c) shielded fabric as ground, (d) measurement setup.

physical contact between patch and ring within same element and the physical contact between elements with large dimensions closed to each other in the array environment. To analyze these problems, a four-elements (2 × 2 array) laid prototype is made, as shown in Figure 26. It consists of the smallest size element, medium size element, largest size element and two largest size elements close to each other. The dimensions of these elements are obtained from the final selected unit cell's (square patch with square ring around it) reflecting phase curve. An overall error of less than 4.7% is observed between required and laid dimensions in ring width, gap and separation between two largest possible elements close-by. The standard C-band waveguide is used for measuring reflection amplitude and phase behavior, so rectangular unit cells are required to simulate and fabricate instead of square cells, which can fit within the waveguide.Four textile based radiating elements are laid using conductive thread in a C-band standard rectangular waveguide unit cell, as shown in Figure 27(a), Figure 27(d). The laid four radiating elements (patch with ring) are 14 mm, 16 mm, 18 mm and 20 mm in size, printed on a 47.55 mm × 22.15 mm rectangular unit cell. A TRL calibration has been used for reference plane adjustment. The reflected amplitude and phase measurements are compared when solid copper ground plane is replaced with the shielded fabric as the ground plane at the bottom of unit cells, as shown in

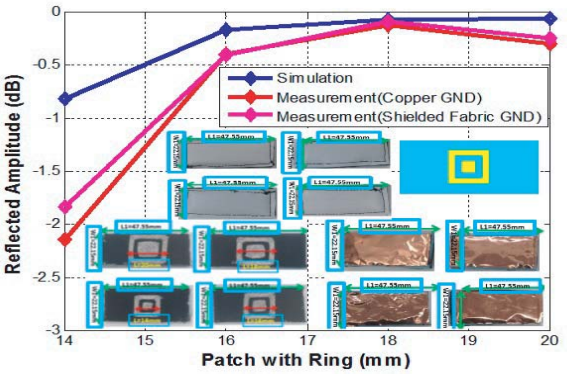

Figure 28. Reflected wave amplitude comparison with element size variation between simulation and measurements using copper and shielded fabric ground plane at 5.8 GHz.

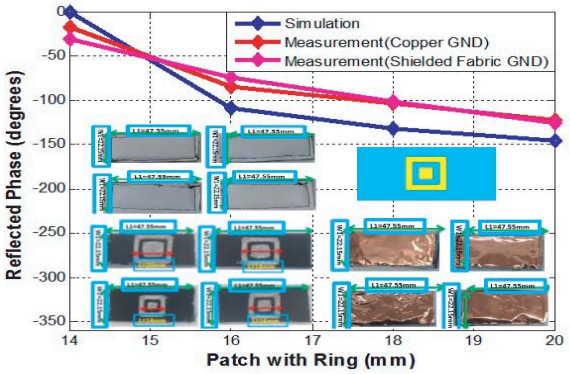

Figure 29. Reflected wave phase comparison with element size variation between simulation and measurements using copper and shielded fabric ground plane at 5.8 GHz.

Figure 27(b) and Figure 27(c). It is clear from the results shown in Figure 28 and Figure 29 that the smaller sized elements reflect higher amplitude losses while 30°–40° reflected phase difference is observed between simulation and measurements. There are multiple factors involved causing these simulation and measurement differences, e.g., the fabrication errors (laid unit cells contain 10% dimension errors), thickness error because of the used soft polyester materials particularly at the borders where stitching is used to attach shielded fabric at the bottom, the ripples in copper ground plane, non-flatness problem due to flexible materials observed during fitting in the waveguide, small air gaps at the corners due to fabricated dimensions error causing energy leakage, etc.

4. CONCLUSION

This paper has presented comprehensive analysis of unit cell in terms of reflected wave amplitude and phase behavior, for designing linearly polarized single-layer Textile-Reflectarray (TRA) at C-band. The use of textile materials in RA antennas makes it attractive due to low weight, cheap price, flexibility and portability. Four fabric samples are selected for the analysis due to material composition and fabrication suitability. The relative permittivity of the material has been extracted using resonance method and a WLAN antenna, IEEE C-band antenna and an antenna with known relative permittivity (foam), has been designed and measured for the validation of extracted relative permittivity. An error of less than 5% is observed in extracted relative permittivity, in most of the measured results of the validation antennas. The extracted dielectric constant is used in unit cell designing of the TRA in the C-band (5.8 GHz). The radiating elements are laid using conductive threads. A square patch with a ring has been selected after analyzing multiple geometries of the patch providing required reflected phase range and low losses. By varying the size of patch and ring of a single-layer unit cell in CST periodic environment, reflected phase range of 360 degrees has been achieved, which is adequate for RA designing. The solid copper ground plane at the bottom of unit cell has been replaced with conductive shielded fabric with high-level signal attenuation. A $2 * 2$ array has been fabricated using conductive thread, for evaluating the possible problems that may occur during large-sized textileRA design. Some important factors, e.g., ring width, gap between ring and patch, the two close-by largest size elements' physical contact and the smallest sized elements accurate laying, are carefully investigated before array laying. A good accuracy, with error less than 5% in required and fabricated dimensions, has been achieved in 2×2 array prototype. Four different standard C-band rectangular waveguide unit cells using conductive thread have been fabricated and measured at 5.8 GHz for reflected amplitude and phase. The solid copper ground plane has been replaced with shielded fabric at the bottom of unit cell, and measurement results are compared with simulation. The proposed method provides motivational step towards designing flexible high gain reflectarrays.

ACKNOWLEDGMENT

The author would like to thank sincerely, from the bottom of his heart, to one of his Fine-Art research group colleague Genevieve Moisan, for her passionate interest in wearable antennas and her countless support in making this project complete and successful.

REFERENCES

1. Huang, J. and J. A. Encircle, *Reflectarray Antennas*, John Wiley & Sons Inc., Hoboken, NJ, 2007.
2. Polar, D. M., S. D. Tarkington, and H. D. Rigors, "Design of millimeter wave microstrip reflectarrays," *IEEE Transactions on Antennas and Propagation*, Vol. 45, No. 2, 287–296, 1997.
3. Haug, J. and R. J. Pozorzelski, "A Ka-band microstrip reflectarray with elements having variable rotation angles," *IEEE Transaction on Antennas and Propagation*, Vol. 46, No. 5, 650–656, May 1998.
4. Malfajani, S. and Z. Atlasbaf, "Design and implementation of a broadband single layer circularly polarized reflectarray antenna," *IEEE Antennas Wireless Propag. Lett.*, Vol. 11, 973–976, Aug. 2012.
5. Carrasco, E., M. Barba, and J. A. Encinar, "Reflectarray element based on aperture-coupled patches with slots and lines of variable length," *IEEE Transaction on Antennas and Propagation*, Vol. 55, No. 3, 820–825, Mar. 2007.
6. Bialkowski, M. E. and K. H. Sayidmarie, "Investigations into phase characteristics of a single-layer reflectarray employing patch or ring elements of variable size," *IEEE Transactions on Antennas and Propagation*, Vol. 56, No. 11, 3366, 3372, Nov. 2008.
7. Mahmoud, A. and A. A. Kishk, "Ka-band dual mode circularly polarized reflectarray," *IEEE Conference ANTEM*, Victoria, Canada, 2014.
8. Encinar, J. A., "Design of two-layer printed reflectarray using patches of variable size," *IEEE Transaction on Antennas and Propagation*, Vol. 49, 1403–1410, 2001.
9. Chaharmir, M. R., J. Shaker, N. Gagnon, and D. Lee, "Design of broadband, single layer dual-band large reflectarray using multi open loop elements," *IEEE Transactions on Antennas and Propagation*, Vol. 58, No. 9, 2875–2883, Sep. 2010.
10. Encinar, J. A. and J. A. Zornoza, "Broadband design of three-layer printed reflectarrays," *IEEE Transaction on Antennas and Propagation*, Vol. 51, No. 7, 1662–1664, Jul. 2003.
11. Pozar, D. M., "Bandwidth of reflectarrays," *IEEE Electronics Letters*, Vol. 39, No. 21, 1490–1491, Oct. 2003.
12. Deguchi, H., K. Mayumi, M. Tsuji, and T. Nishimura, "Broadband single-layer triple-resonance microstrip reflectarray antennas," *Proc. EuMA*, 29–32, Italy, 2009.
13. Hasani, H., M. Kamyab, and A. Mirkamali, "Broadband reflectarray antenna incorporating disk elements with attached phase-delay lines," *IEEE Antennas and Wireless Propagation Letters*, Vol. 9, 156–158, 2010.
14. Koski, K., L. Sydanheimo, Y. Rahmat-Samii, and L. Ukkonen, "Fundamental characteristics of electro-textiles in wearable UHF RFID patch antennas for body-centric sensing systems," *IEEE Transactions on Antennas and Propagation*, Vol. 62, No. 12, 6454, 6462, Dec. 2014.
15. Matthew, J. C. G., B. Pirollo, A. Tyler, and G. Pettitt, "Body wearable antennas for UHF/VHF," *Loughborough Antennas and Propagation Conference (LAPC), 2008*, 357, 360, Mar. 17–18, 2008.
16. Zhang, S., A. Chauraya, W. Whittow, R. Seager, T. Acti, T. Dias, and Y. Vardaxoglou, "Embroidered wearable antennas using conductive threads with different stitch spacings," *Loughborough Antennas and Propagation Conference (LAPC), 2012*, 1, 4, Nov. 12–13, 2012.
17. Subramaniam, S., S. Dhar, K. Patra, B. Gupta, L. Osman, K. Zeouga, and A. Gharsallah, "Miniaturization of wearable electro-textile antennas using Minkowski fractal geometry," *2014 IEEE Antennas and Propagation Society International Symposium (APSURSI)*, 309, 310, Jul. 6–11, 2014.

18. Jiang, Z. H., D. E. Brocker, P. E. Sieber, and D. H. Werner, "A compact, low-profile metasurface-enabled antenna for wearable medical body-area network devices," *IEEE Transactions on Antennas and Propagation*, Vol. 62, No. 8, 4021, 4030, Aug. 2014.
19. Rahmat-Samii, Y., "Wearable and implantable antennas in body-centric communications," *The Second European Conference on Antennas and Propagation, 2007. EuCAP 2007*, 1, 5, Nov. 11–16, 2007.
20. Salonen, P., K. Jaehoon, and Y. Rahmat-Samii, "Dual-band E-shaped patch wearable textile antenna," *2005 IEEE Antennas and Propagation Society International Symposium*, Vol. 1A, 466, 469, Jul. 3–8, 2005.
21. Moukanda, M., F. Ndagijimana, J. Chilo, and P. Saguet, "A coaxial probe fixture used for extracting complex permittivity of thin layers," *IEEE Annual Wireless and Microwave Technology Conference, 2006. WAMICON'06*, 1–4, Dec. 4–5, 2006.
22. Baginski, M. E., D. L. Faircloth, and M. D. Deshpande, "Comparison of two optimization techniques for the estimation of complex permittivities of multilayered structures using waveguide measurements," *IEEE Transactions on Microwave Theory and Techniques*, Vol. 53, No. 10, 3251–3259, Oct. 2005.
23. Moukanda, F. M., F. Ndagijimana, J. Chilo, and P. Saguet, "A cavity in transmission for extracting electric parameters of thin layers," *International Symposium on Signals, Systems and Electronics, 2007. ISSSE'07*, 431–434, Jul. 30–Aug. 2, 2007.
24. Haddadi, K. and T. Lasri, "Geometrical optics-based model for dielectric constant and loss tangent free-space measurement," *IEEE Transactions on Instrumentation and Measurement*, Vol. 63, No. 7, 1818–1823, Jul. 2014.
25. Sankaralingam, S. and B. Gupta, "Determination of dielectric constant of fabric materials and their use as substrates for design and development of antennas for wearable applications," *IEEE Transactions on Instrumentation and Measurement*, Vol. 59, No. 12, 3122, 3130, Dec. 2010.
26. Shams, S. I., M. M. Tahseen, and A. A. Kishk, "Relative permittivity extraction of textile materials based on ridge gap waveguide technology," *IEEE Symposium on Antennas and Propagation and URSI (APS/URSI)*, Vancouver, BC, Canada, Jul. 19–25, 2015.
27. http://www.lessemf.com/, 776-B Watervliet Shaker Rd, Latham, NY 12110, USA.